Elimination of spiral chaos by pulse entrainment in the Aliev-Panfilov model

Hidetsugu Sakaguchi and Yusuke Kido
Department of Applied Science for Electronics and Materials, Interdisciplinary Graduate School of Engineering Sciences, Kyushu University, Kasuga, Fukuoka, Japan

(Received 20 December 2004; revised manuscript received 9 February 2005; published 19 May 2005)

Pulse entrainment between two excitatory media is studied in the Aliev-Panfilov model. We show that a spiral chaos in the continuous excitatory medium can be eliminated by a grid network using the pulse entrainment. This mechanism may be applied to the cardiac system, where the ventricular fibrillation is interpreted as the spiral chaos and the Purkinje fibers act as the grid network.

DOI: 10.1103/PhysRevE.71.052901 PACS number(s): 87.19.Hh, 05.45.Xt, 89.75.Kd

Some types of cardiac arrhythmia are considered to be related to spiral waves in excitable media [1–3]. The ventricular fibrillation is a serious cardiac arrhythmia, which leads to sudden death by heart attacks. Irregular and fast oscillations are seen in the electrocardiogram when the ventricular fibrillation occurs. In normal states, the excitation pulses propagate, starting from the sinoatrial node, via the atrial-ventricular node, through the Purkinje fibers to the ventricular cells. In the ventricular fibrillation, excitation waves are generated from regions other than the sinoatrial node and propagate irregularly. The detailed mechanism of the ventricular fibrillation is not known well, but the irregular time evolution of activity might be due to the spiral chaos in the excitable system.

There are some model equations for the cardiac cells based on the dynamics of ion channels [4,5]. Some methods to control the spiral chaos were proposed, using the model equations [6,7]. Those model equations are rather complicated. We use the Aliev-Panfilov model [8] to study the spiral chaos and its control. This model is a phenomenological model with two variables like the FitzHugh-Nagumo model for a neuron. The model equation is expressed as

$$\frac{\partial e}{\partial t} = -Ke(e-a)(e-1) - er + D\nabla^2 e,$$

$$\frac{\partial r}{\partial t} = [\epsilon + \mu_1 r/(\mu_2 + e)][-r - ke(e-b-1)], \qquad (1)$$

where e denotes a variable representing the membrane potential, and r is a variable related to ion channels. The excitation wave of the ventricular cells has a rather long plateau and the width of the plateau strongly depends on the pulse interval. The Aliev-Panfilov model is constructed to reproduce the above characteristics qualitatively. The parameters other than a and D are fixed to be $K=8$, $\epsilon=0.01$, $\mu_1=0.11$, $\mu_2=0.3$, and $b=0.1$. In the one-dimensional system, there are pulse-train solutions (periodic waves). The pulse-train solutions become unstable if the parameter a is below a critical value a_c. The pulse width of the excitable pulse begins to oscillate below the critical value. This is the breathing instability of the pulse trains, and it is also called the alternans instability [9]. When the breathing instability is sufficiently strong, the pulse train collapses. If this type of collapse of pulse trains occurs in a spiral pattern, the spiral collapses and another spiral is spontaneously created, and it leads to a spiral chaos [10]. The spiral chaos appears for $a \leqslant 0.115$. We have proposed a method of elimination of the spiral chaos by periodic forcing [11]. (Alonso *et al.* studied the supression of turbulence of scroll waves by periodic forcing in the Barkley model [12].)

The real heart is not a homogeneous system such as the Aliev-Panfilov equation. There are various structures and inhomogeneities. We consider mainly the effect of the Purkinje fibers in this paper. The Purkinje fibers make a network structure. The excitation pulse propagates several times faster in the Purkinje fibers than in the normal ventricular tissue. For simplicity, we assume that the dynamics of the Purkinje fibers is represented by the same model equation (1) with larger D (D is assumed to be 1 in the ventricular tissue), since the pulse velocity is proportional to $\sqrt{D}$. We consider a two-layer model of the Aliev-Panfilov equation. The first layer represents the ventricular tissue and the second layer

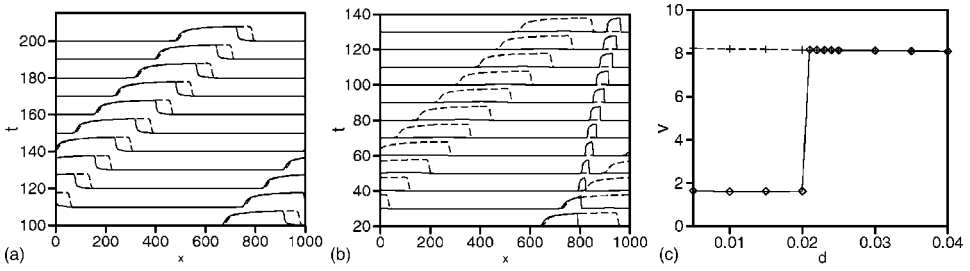

FIG. 1. (a) Entrainment of two pulses at $d=0.03$. The solid lines denote $e_1(x,t)$ and the dashed lines denote $e_2(x,t)$. (b) Desynchronization of two pulses at $d=0.02$ in the coupled one-dimensional Aliev-Panfilov model. (c) Pulse velocities in the first fiber (rhombi) and in the second fiber (crosses) as a function of d.

the Purkinje fibers, assuming that the Purkinje fiber network covers on the ventricular tissue. First, we study the pulse entrainment between the two fibers with a one-dimensional model. The model equation is written as

$$\frac{\partial e_1}{\partial t} = -Ke_1(e_1-a)(e_1-1) - e_1 r_1 + \frac{\partial^2 e_1}{\partial x^2} + d_{12}(e_2-e_1),$$

$$\frac{\partial r_1}{\partial t} = [\epsilon + \mu_1 r_1/(\mu_2+e_1)][-r_1 - ke_1(e_1-b-1)],$$

$$\frac{\partial e_2}{\partial t} = -Ke_2(e_2-a)(e_2-1) - e_2 r_2 + D\frac{\partial^2 e_2}{\partial x^2} + d_{21}(e_1-e_2),$$

$$\frac{\partial r_2}{\partial t} = [\epsilon + \mu_1 r_2/(\mu_2+e_2)][-r_2 - ke_2(e_2-b-1)], \quad (2)$$

where e_1 and e_2 represent, respectively, the membrane potentials in the first and second fibers, and d_{12} is a coupling constant from the second fiber to the first fiber, and d_{21} is a coupling constant from the first fiber to the second fiber. We do not always assume the symmetry $d_{12}=d_{21}$, considering situations such that the membrane potentials change differently in the two fibers owing to the difference of the thickness. The pulse propagates faster by $\sqrt{D}$ in the second fiber than in the first fiber, if $d_{12}=d_{21}=0$. The interaction between the two fibers induces the entrainment of pulse propagation.

Figure 1(a) displays the time evolutions of $e_1(x,t)$ [solid line] and $e_2(x,t)$ [dashed line] for $d_{12}=d_{21}=d=0.03$ and $D=25$. The system size is $L=1000$ and the periodic boundary conditions are assumed. We have used the finite difference method with $\Delta t=0.0005$ and $\Delta x=0.5$. The two pulses propagate with the same velocity, therefore, we can say that the two pulses are mutually entrained. Figure 1(b) displays the time evolutions of $e_1(x,t)$ (solid line) and $e_2(x,t)$ (dashed line) for $d_{12}=d_{21}=d=0.02$ and $D=25$. The mutual coupling is weak and the slower pulse described by $e_1(x,t)$ cannot follow the second pulse. Indeed, the velocity of the first pulse becomes nearly one-fifth of that of the second pulse. Figure 1(c) displays the pulse velocities of the two pulses. The pulse entrainment breaks down below $d=0.02$ if the coupling constants d_{12} and d_{21} take the same value d. Below $d=0.02$, the pulse velocities take two different values in the first and second fibers, which are almost the same as two pulse velocities in the case of no coupling. Above $d=0.02$, the pulse entrainment occurs, the pulse velocities take the same value in the first and second fibers, which is almost the same as the pulse velocity in the second (faster) fiber. (In contrast, Monine *et al.* found that a slower front dominates the front propagation in a problem of coupled layers in surface catalysis [13].)

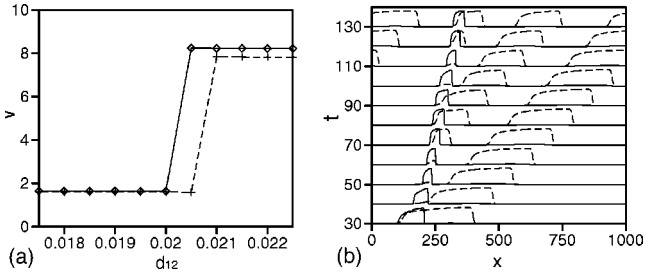

FIG. 2. (a) Pulse velocities in the first fiber as a function of d_{12} for $d_{21}=0$ (rhombi) and 0.1 (crosses). (b) Time evolutions of e_1 (solid line) and e_2 (dashed line) for $d_{21}=0.1$ and $d_{12}=0.018$.

Similar behaviors are obtained for more general cases of asymmetric coupling. Figure 2(a) displays the velocities of the pulse in the first as a function of d_{12} for $d_{21}=0$ (rhombi) and $d_{21}=0.1$ (crosses). The case of $d_{21}=0$ represents the one-way coupling, since the second fiber is not affected by the first fiber. The pulse velocity in the first fiber jumps at a critical value d_{12c}, and the pulse entrainment occurs for $d_{12} \geqslant d_{12c}$. The critical value d_{12c} is nearly 0.020 for $d_{21}=0$ and $d_{12c} \sim 0.0205$ for $d_{21}=0.1$. The critical value d_{12c} is nearly 0.20, and hardly depends on d_{21}. The velocity of the pulse in the first fiber jumps down discontinuously below the critical coupling. For $d_{21}=0.1$, the interaction from the first fiber to the second fiber is stronger, then, the delayed pulse in the first fiber excites another pulse in the second fiber. As a result, the slower pulse in the first fiber becomes a generator of pulses in the second fiber. Figure 2(b) displays such a time evolution of the pulse generation at $d_{21}=0.1$ and $d_{12}=0.018$. Pulses are generated periodically in the second fiber, and the period is 41.4 for $d_{21}=0.1$ and $d_{12}=0.018$.

Next, we study two-dimensional systems. The Purkinje fibers make a complicated network structure, but here we have assumed a grid structure of mesh-size 20 for the network in the second layer for the sake of simplicity. We consider a coupled system in which the grid network is surmounted on a normal plane. Our model equation is almost the same as Eq. (2), but $\partial^2/\partial x^2$ is replaced by the Laplacian ∇^2. The variables e_1 and r_1 in the first layer are defined

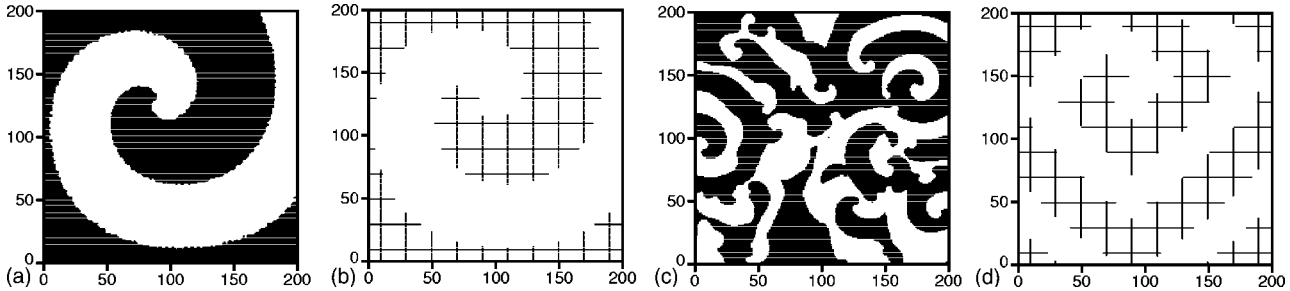

FIG. 3. (a), (b) Initial patterns of e_1 (a) and e_2 (b) for the numerical simulation. (c), (d) Snapshot patterns of e_1 (c) and e_2 (d) for $a=0.1$, $D=4$, $d_{12}=0$, and $d_{21}=0$. In the marked region, e_1 (e_2) satisfies $e_1>0.4$ ($e_2>0.4$). A spiral chaos apppears in the first layer, but a spiral pattern is stable in the second layer.

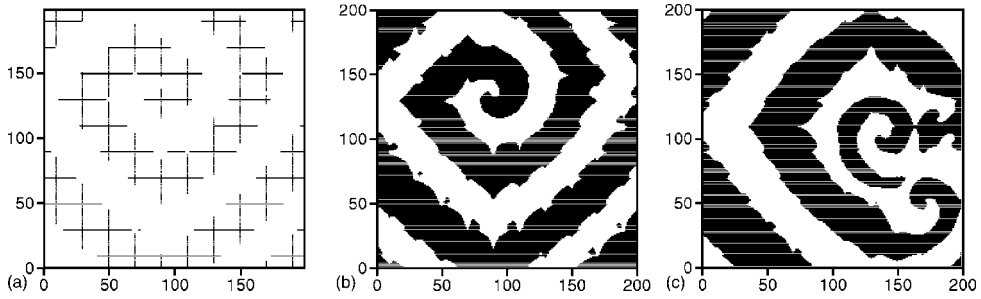

FIG. 4. (a), (b) Snapshot patterns of e_2 (a) and e_1 (b) for $a=0.1$, $D=4$, $d_{12}=1$, and $d_{21}=0.1$. In the marked region, e_2 (e_1) satisfies $e_2>0.4$ ($e_1>0.4$). A stable spiral appears in the second layer, and a regular spiral appears also in the first layer as a result of the mutual synchronization. (c) Snapshot pattern of e_1 for $a=0.1$, $D=4$, $d_{12}=1$, and $d_{21}=0.3$. A spiral is unstable and many spirals are created.

on a normal two-dimensional plane, and e_2 and r_2 in the second layer are defined only on the grid lines satisfying $x=20i+10$ or $y=20j+10$ where i and j are integers. The Laplacian $\nabla^2 e_2$ is calculated in the second layer as $\partial^2 e_2/\partial x^2$ or $\partial^2 e_2/\partial y^2$ on the grid lines other than the intersections $(20i+10, 20j+10)$ and it is calculated as $\partial^2 e_2/\partial x^2+\partial^2 e_2/\partial y^2$ at the intersections. We have used the finite difference method with $\Delta=0.0005$ and $\Delta x=0.5$ also in the two-dimensional simulations.

We consider the cases of relatively stronger interaction, where the excitation waves tend to be synchronized between the two layers. However, several types of excitation waves, such as regular one-dimension pulses, spiral waves, and spiral chaos, propagate in two dimensions. We investigate which types of excitation waves appear in the coupled systems. A spiral pattern is unstable for $a<0.115$ in the first layer, if there is no interaction, i.e., $d_{12}=0$ and $d_{21}=0$. However, a stable spiral appears on a grid structure in the second layer. We first show a numerical simulation for $a=0.1$ and $D=4$ in the case of no coupling. Figures 3(a) and 3(b) show initial patterns for e_1 and e_2. The initial values are the same on the grid lines, i.e., $e_1(x,y)=e_2(x,y)$. Figure 3(c) displays a spiral chaos in the first layer. The initial regular spiral breaks up and many small spirals are created. Figure 3(d) displays a stable spiral in the second layer. The spiral is rather angular because it appears on the grid structure. It is not a numerical artifact. We have got the same angular spiral even in a simulation with higher resolution with smaller space step Δx. We have checked that this type of spiral is stable even for $a=0.06$ in the grid network. The average period of temporal oscillation is 29.4 in the first layer, and the period of oscillation is 34.5 in the second layer. The spiral in Fig. 3(d) rotates slower than the spiral chaos in Fig. 3(c). If the mutual interaction is not zero, mutually synchronized spiral waves can appear. Figures 4(a) and 4(b) display snapshot patterns of (a) e_2 and (b) e_1 at the same time for $a=0.1$, $D=4$, $d_{21}=0.1$, and $d_{12}=1$. A spiral rotates stably in the first layer, which is entrained to the spiral in the second layer. The initial condition is a regular spiral shown in Figs. 3(a) and 3(b). The stable spiral in the second layer overcomes the spiral chaos in the first layer owing to the asymmetric coupling $d_{21}<d_{12}$. If d_{21} is step by step increased at a fixed value of $d_{12}=1$, the spiral becomes unstable at $d_{21}\sim 0.27$ and many spirals are created. Figure 4(c) displays a snapshot pattern of e_1 in the first layer for $a=0.1$, $D=4$, $d_{21}=0.3$, and $d_{12}=1$. At the parameter, spirals are created also in the second layer, but the motion is almost synchronized between the two layers. That is, the spiral chaos in the first layer dominates the whole system for relatively larger d_{21}.

Even if the initial condition is a spiral chaos in the first layer and a regular spiral in the second layer, the regular spiral in the second layer can entrain the whole system for sufficiently small d_{21}. For this type of simulation, we have assumed that the initial condition for e_2 is a regular spiral shown in Fig. 3(d) and the initial condition for e_1 is a spiral chaos shown in Fig. 3(c). Figure 5(a) displays a snapshot pattern of e_1 for $a=0.1$, $D=4$, $d_{12}=1$, and $d_{21}=0.06$. The initial spiral chaos is eliminated and a regular spiral appears in the first layer. Figure 5(b) displays a snapshot pattern of e_1 for $a=0.1$, $D=4$, $d_{12}=1$, and $d_{21}=0.08$. The spiral chaos cannot be eliminated, and the spiral chaos in the first layer dominates the whole system. The transition for the elimination of the spiral chaos occurs at $d_{21}\sim 0.07$ for $a=0.1$, $D=4$, and $d_{12}=1$. This critical value of d_{21} is different from the critical value of the instability of a regular spiral as shown in Fig. 4. Even a smaller value of d_{21} is necessary for the elimination of the initial spiral chaos. Thus we have shown that the spiral chaos is eliminated in the first layer (corresponding to the ventricular cells) by the regular spiral in the second layer (corresponding to the Purkinje fibers), if the coupling is sufficiently asymmetric. We have shown the results only for $D=4$ and $a=0.1$, but similar results are observed for other parameters.

The elimination of the spiral chaos in the first layer can be

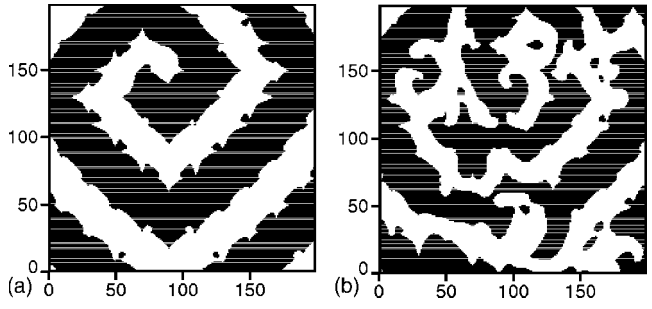

FIG. 5. (a) Snapshot pattern of e_1 for $a=0.1$, $D=4$, $d_{12}=1$, and $d_{21}=0.06$. As an initial condition, a regular spiral is set in the second layer and a spiral chaos is set in the first layer. The spiral chaos is eliminated. (b) Snapshot pattern of e_1 for $a=0.1$, $D=4$, $d_{12}=1$, and $d_{21}=0.08$. A spiral chaos dominates the whole system.

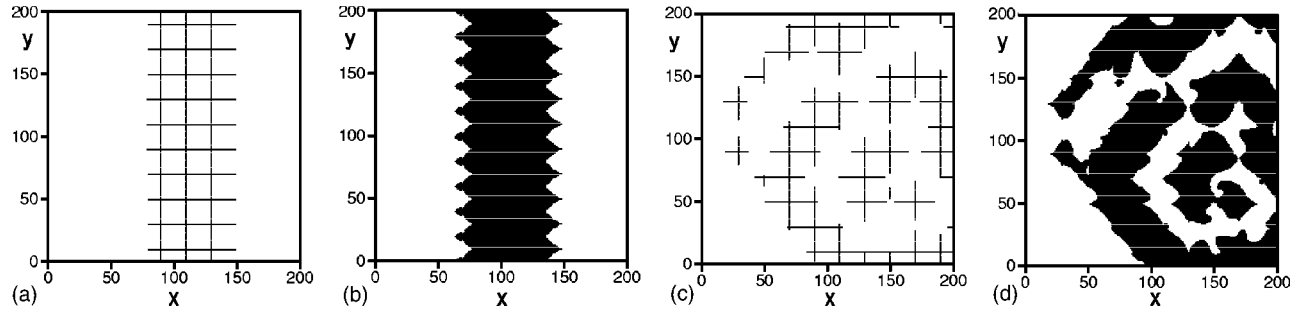

FIG. 6. (a), (b) Snapshot patterns of e_2 (a) and e_1 (b) for $a=0.1$, $D=4$, $d_{21}=0.15$, and $d_{12}=4$ with a pacemaker region in the left side of the second layer. The spiral chaos is eliminated and a regular pulse is propagating in the $+x$ direction in both layers. (c), (d) Snapshot patterns of e_2 (c) and e_1 (d) for $a=0.1$, $D=4$, $d_{21}=0.19$, and $d_{12}=4$. Spiral chaos dominates in both layers.

performed even by regular pulses in the second layer. In normal states of heart beating, regular pulses are emitted from a pacemaker region and propagate through the Purkinje fibers. The regular pulses are transmitted to the ventricular cells. To simulate a similar situation, we have performed a numerical simulation. To generate regular pulses in the second layer, a periodic force of the form $f=0.2\sin(2\pi t/60)$ is applied in the region $x<10$, and $e_2(x,y)=0$ is assumed initially in the second layer. In this simulation, the region $x<10$ in the second layer works as a pacemaker region. The period 60 is rather smaller than the period of spiral waves. If the initial condition of e_1 is 0 in the first layer, regular pulses propagate naturally both in the first and second layers. To test a possibility of the elimination of the spiral chaos in the first layer by the regular pulses in the second layer, the initial condition of e_1 is set to be a spiral chaos shown in Fig. 3(c), and the initial condition of e_2 is set to be a regular pulse state constructed by a simulation without the mutual coupling. Figures 6(a) and 6(b) display snapshot patterns of (a) e_2 and (b) e_1 for $a=0.1$, $D=4$, $d_{21}=0.15$, and $d_{12}=4$. A regular pulse propagates in the $+x$ direction in both layers. The spiral chaos in the first layer is eliminated and the periodic forcing in the pacemaker region dominates the whole system. If this type of phenomenon occurs in real hearts, the ventricular fibrillation can be eliminated by the regular pulses through the Purkinje fibers starting from the pacemaker region in the sinoatrial node. Figures 6(c) and 6(d) display snapshot patterns of e_2 and e_1 for $a=0.1$, $D=4$, $d_{21}=0.19$, and $d_{12}=4$. The spiral chaos cannot be eliminated at the parameter and almost synchronized spiral chaos appears in both layers. The transition for the elimination of the spiral chaos occurs at $d_{21}\sim 0.17$ for $a=0.1$, $D=4$, and $d_{12}=4$. The critical value of d_{21} increases with $\sqrt{D}$ for $a=0.1$ and $d_{12}=4$. For example, the critical values of d_{21} are evaluated as $d_{21c}=0.09$ for $\sqrt{D}=1$, $d_{21c}=0.17$ for $\sqrt{D}=2$, $d_{21c}=0.34$ for $\sqrt{D}=4$, $d_{21c}=0.46$ for $\sqrt{D}=6$, and $d_{21c}=0.6$ for $\sqrt{D}=8$. That is to say, the elimination of spiral chaos occurs more easily as $\sqrt{D}$ is increased. The pulse velocity increases in proportion to $\sqrt{D}$ if the interaction between the two layers is absent. If the sinusoidal force $f=0.2\sin(2\pi t/60)$ is uniformly given to the grid network in the second layer, the elimination of the spiral chaos occurs below $d_{21}=2.0$, when d_{12} is fixed to be 4. This simulation corresponds to the case of $D\to\infty$. Thus we have found that the regular pulses in the second layer (corresponding to the Purkinje fibers) cause the pulse entrainment between the two layers, and the spiral chaos can be eliminated, if the coupling is sufficiently asymmetric. The strong effect of the Purkinje fibers on the ventricular cells may be related to the suppression of the ventricular fibrillation.

[1] J. Davidenko, A. Pertsov, R. Salomonsz, W. Baxter, and J. Jalife, Nature (London) **355**, 349 (1993).
[2] R. A. Gray, A. M. Pertsov, and J. Jalife, Nature (London) **392**, 75 (1998).
[3] F. X. Witkowsku, L. J. Leon, P. A. Penkoske, W. R. Giles, M. L. Spano, W. L. Ditto, and A. T. Winfree, Nature (London) **392**, 78 (1998).
[4] G. Beeler and H. Reuter, J. Physiol. (London) **268**, 1 (1977).
[5] F. Fenton and A. Karma, Chaos **8**, 20 (1998).
[6] W. J. Rappel, F. Fenton, and A. Karma, Phys. Rev. Lett. **83**, 456 (1999).
[7] D. Allexandre and N. F. Otani, Phys. Rev. E **70**, 061903 (2004).
[8] R. R. Aliev and A. V. Panfilov, Chaos, Solitons Fractals **7**, 293 (1996).
[9] M. Courtemanche, L. Glass, and J. P. Keener, Phys. Rev. Lett. **70**, 2182 (1993).
[10] A. V. Panfilov, Phys. Rev. Lett. **88**, 118101 (2002).
[11] H. Sakaguchi and T. Fujimoto, Phys. Rev. E **67**, 067202 (2003).
[12] S. Alonso, F. Sagués, and A. S. Mikhailov, Science **299**, 1722 (2003).
[13] M. Monine, L. Pismen, M. Bär, and M. Or-Guil, J. Chem. Phys. **117**, 4473 (2002).